Journal of Chromatography, 186 (1979) 117–127

CHROM. 12,022

CHROMATOGRAPHIC PEAK SHAPE

III. INFLUENCE OF KINETICS PARAMETERS ON SOLUTE PROFILES

ELI GRUSHKA and SANDRA D. MOTT
Department of Chemistry, State University of New York at Buffalo, Buffalo, N.Y. 14214 (U.S.A.)

SUMMARY

The eight parameters of the Chesler–Cram equation are examined in order to relate them to chromatographic processes. For this purpose Giddings' stochastic theory is used to generate peaks which are then least square fitted to the Chesler–Cram equation. The dependence of the Chesler–Cram parameters on the adsorption–desorption rate constants is observed. It is found that, while some peculiarities do exist, in general the behavior of the empirical parameters can be related to these rate constants. Moreover, the study seems to indicate that the Chesler–Cram equation can be used to extract the rate constants from experimental peaks.

INTRODUCTION

In previous communications concerning chromatographic peak shape[1,2], we have examined the validity and the practical usefulness of the Chesler–Cram model[3]. This model is based on the following eight parameters, C_1–C_8, empirical equation

$$Y(t) = C_1[A + (1 - 0.5B)(C)] \quad (1)$$

where

$$A = \exp\left[\frac{-(t - C_4)^2}{2C_5}\right]$$
$$B = 1 - \tanh[C_2(t - C_3)]$$
$$C = C_6 \exp[-0.5C_7(|t - C_8| + t - C_8)]$$

The parameters C_1–C_8 have the following meaning. C_1 is the peak maximum; C_2 is the slope of the hyperbolic tangent at time equal to C_3; C_3 is the position (in time)

of the midpoint of the hyperbolic tangent; C_4 is the position (in time) of the peak maximum; C_5 is the variance of the Gaussian portion of the peak profile; C_6 is the height ratio of the maximum of the exponential decay to C_1 at time C_8; C_7 is the rate of the exponential decay; C_8 is the position (in time) where the decay function originates. Eqn. 1 is made up of three terms: a Gaussian (term A), an exponential decay (term C) and an hyperbolic tangent joining function (term B).

We have shown previously that (a) experimental data can be described by the Chesler–Cram model, (b) some of the parameters of the model are related to mass transfer processes and (c) statistical moments of the elution profiles can be obtained with very good precision when the model is fitted to the experimental data.

The Chesler–Cram equation is quite successful as a fitting model to experimental chromatograms, perhaps due to the fact that it is an eight parameter equation. Because of the ease in manipulating the model, it would be of interest to see the connection between the fitting parameters and the chromatographic processes which occur in the column. Toward this aim, we shall choose a theoretical concentration profile, generate with it peaks, and fit them to the Chesler–Cram equation. By observing the dependence of the C_1–C_8 parameters on the theoretical equation, we can determine their physical significance.

THEORY

Among the several available theoretical concentration profiles, the one which contains the most information is that described by Giddings and co-workers[4–7], and independently by McQuarrie[8], using stochastic arguments. The model, which is particularly suitable for describing tailing peaks, is based on the presence of high energy adsorption sites which retain the solute to a greater degree than other chromatographic processes such as partitioning or rapid desorption. Slow desorptions from the support produce a tail, while the fast exchange phenomena are associated with a Gaussian profile. The contribution of the slow desorption to the peak shape is given by the following expression:

$$P(y) = \left(\frac{A_1 A_2}{y}\right)^{1/2} I_1\left(\sqrt{4A_1A_2y}\right)\left[\exp\left(-A_1 - A_2y\right)\right] \tag{2}$$

where $A_1 = k_a t_m$, $A_2 = k_d t_m$, $Y = (t - t_m - t_s)/t_m$, $I_1(\sqrt{x})$ is a Bessel function of an imaginary argument, k_a and k_d are adsorption and desorption rate constants respectively, t_m is the hold-up time, t_s is the time spent by the solute molecules on the high energy tail producing sites and t is the time coordinate. The fast exchange processes can be expressed by the function $P_f(y)$:

$$P_f(y) = \exp(-A_1)\delta(y) \tag{3}$$

where A and y are as defined above and $\delta(y)$ is the Dirac delta function.

A summation of eqns. 2 and 3 gives the concentration profile of a solute undergoing slow and fast exchange processes. To be physically meaningful, an effective diffusion process (owing to molecular diffusion, to flow heterogeneity, etc.) must be superimposed on the above two processes. Giddings[6] has used the

Schmidt method in order to take into account the diffusion processes. In the present work, a Gaussian, whose variance is proportional to the effective diffusion coefficient, is convoluted with the expressions in eqns. 2 and 3. A similar approach was taken by McQuarrie[8]. The convolution which is determined numerically, is more descriptive of the physical phenomena than the iterative Schmidt method. When the effect of the diffusion processes is taken into account, the theoretical chromatographic elution profile is obtained. To study the relationship between C_1–C_8 and A_1 and A_2, theoretical peaks are generated and are fitted to the Chesler–Cram model.

Recently, Vidal-Madjar and Guiochon[9] have shown that Giddings' stochastic approach can be used with experimental data. They have fitted portions of chromatographic peaks to the theoretical profile and have extracted adsorption–desorption constants. To our knowledge, this is the only attempt to utilize the stochastic model to experimental peaks. Their procedure, however, used an arbitrary assumption to decide the point at which the tail begins.

PROCEDURE

All chromatographic peaks were simulated on a CDC Cyber 173 computer from eqns. 2 and 3. For peak generation, the following parameter values were used. Study 1: $t_s = 90$ sec, $t_m = 10$ sec and number of plates $N = 1000$; study 2: $t_m =$ 5 sec, all other quantities same as in study 1. The theoretical plate number gives the effective diffusion coefficient. The values of the parameters are similar to those used by Giddings. Series of peaks were generated in which A_1 or A_2 were varied.

The generated peaks were treated as experimental data and were fitted to the Chesler–Cram equation using the same algorithm described in ref. 1.

RESULTS AND DISCUSSION

Considering the two sorption parameters, A_1 and A_2, the one likely to exhibit its influence most profoundly is A_2 which reflects desorption. This can be accounted for by inspecting eqn. 2, where in the exponential term the quantity A_2 is multiplied by the dimensionless time y. It can be shown that A_2 controls the length of the tail while A_1 determines its relative height. This is so since A_1 is proportional to the fraction of molecules which are not adsorbed on the tail producing sites:

$$\text{fraction of solute not on high energy sites} = e^{-A_1} \tag{4}$$

Referring back to the empirical equation of Chesler and Cram[3], the parameters which describe the tail of the profile are C_2, C_3, C_6, C_7 and C_8. Therefore, changes in A_2 and A_1 should involve a change in the Chesler–Cram parameters. The dependence of C_2, C_3, C_6, C_7 and C_8 on A_1 and A_2 should illustrate the physical significance of the former quantities.

The following discussion is based on generated peaks with A_1 values in the range of 0.2–1.2 and A_2 values between 1.5 and 4.4. Tables I–IV show only a representative sample of the data obtained. In addition to C_1–C_8, the skew was calculated for each peak and is shown in the tables. The behavior of the skew is quite interesting since it is not a monotonic function of A_1 or A_2. In fact, the skew goes through a

TABLE I

THE CHESLER–CRAM PARAMETERS FOR $A_1 = 0.20$ AND $t_m = 10$ sec

A_2	C_1	C_2	C_3	C_4	C_5	C_6	C_7	C_8	*Skew*
1.581	0.0846	0.4663	104.2	100.9	11.31	0.2755	0.1377	109.5	1.39
1.897	0.0891	0.4757	104.1	100.9	11.32	0.2509	0.1615	109.3	1.35
2.214	0.0930	0.4884	104.0	100.9	11.31	0.2257	0.1845	109.1	1.25
2.530	0.0965	0.3254	106.6	100.9	11.27	0.6409	0.2234	104.3	1.13
2.846	0.0994	0.3265	106.7	100.9	11.23	0.6470	0.2497	104.3	0.997
3.162	0.102	0.3314	106.8	100.9	11.19	0.6559	0.2742	104.2	0.871
3.479	0.104	0.3312	106.9	100.9	11.10	0.6729	0.2999	104.2	0.757
3.795	0.106	0.3382	106.9	100.8	11.06	0.6781	0.3220	104.0	0.696
4.111	0.108	0.3415	107.0	100.8	11.01	0.6763	0.3451	104.0	0.569
4.427	0.109	0.3498	107.0	100.8	10.97	0.6745	0.3642	103.9	0.495

maximum as A_2 is increased and A_1 is kept constant or *vice versa*. This was unexpected since as A_2 increases or as A_1 decreases the importance of the tail diminishes (although as mentioned before for different reasons). The skew was calculated numerically from the generated data rather than obtained analytically from eqns. 2 and 3, and therein might lie the difficulties. In general, however, the skew does decrease as A_2 increases or as A_1 decreases.

TABLE II

THE CHESLER–CRAM PARAMETERS FOR $A_1 = 1.0$ AND $t_m = 10$ sec

A_2	C_1	C_2	C_3	C_4	C_5	C_6	C_7	C_8	*Skew*
1.581	0.0643	0.4362	105.0	101.4	12.33	0.4462	0.1004	110.9	1.04
1.897	0.0696	0.4505	105.0	101.5	12.34	0.4057	0.1204	110.8	1.12
2.214	0.0744	0.4592	104.9	101.5	12.41	0.3711	0.1395	110.5	1.16
2.530	0.0788	0.4718	104.8	101.5	12.37	0.3366	0.1586	110.3	1.15
2.846	0.0825	0.4775	104.6	101.5	12.23	0.3105	0.1762	110.0	1.11
3.162	0.0861	0.4881	104.6	101.5	12.16	0.2814	0.1936	109.9	1.04
3.479	0.0893	0.4979	104.5	101.5	12.09	0.2553	0.2101	109.7	0.969
3.795	0.0922	0.5068	104.4	101.5	12.01	0.2318	0.2257	109.6	0.889
4.111	0.0946	0.5069	104.4	101.4	11.87	0.2157	0.2386	109.3	0.811
4.427	0.0970	0.3201	107.5	101.4	11.80	0.8775	0.2907	104.8	0.737

TABLE III

THE CHESLER–CRAM PARAMETERS FOR $A_1 = 0.2$ AND $t_m = 5$ sec

A_2	C_1	C_2	C_3	C_4	C_5	C_6	C_7	C_8	*Skew*
1.581	0.1118	0.3489	101.1	95.54	9.708	0.5126	0.2768	98.66	0.961
1.897	0.1153	0.3572	101.2	95.53	9.675	0.5360	0.3250	98.55	0.716
2.214	0.1181	0.3682	101.3	95.52	9.635	0.5482	0.3682	98.43	0.536
2.530	0.1203	0.3806	101.4	95.50	9.594	0.5486	0.4062	98.30	0.407
2.846	0.1221	0.3887	101.5	95.48	9.553	0.5425	0.4443	98.26	0.314
3.162	0.1234	0.3979	101.4	95.46	9.499	0.5492	0.4761	98.11	0.247
3.479	0.1247	0.4105	101.4	95.44	9.464	0.5309	0.5228	97.99	0.198
3.795	0.1257	0.4180	101.4	95.42	9.431	0.5178	0.5331	97.96	0.161
4.111	0.1265	0.4300	101.4	95.40	9.401	0.4982	0.5549	97.85	0.133
4.427	0.1273	0.4374	101.4	95.39	9.374	0.4898	0.5840	97.83	0.112

TABLE IV

THE CHESLER–CRAM PARAMETERS FOR $A_1 = 1.0$ AND $t_m = 5$ sec

A_2	C_1	C_2	C_3	C_4	C_5	C_6	C_7	C_8	*Skew*
1.581	0.09396	0.5117	98.96	95.98	10.41	0.2590	0.1947	104.0	1.16
1.897	0.09938	0.5270	98.85	95.99	10.36	0.2220	0.2272	103.7	0.993
2.214	0.1039	0.3387	101.7	95.98	10.30	0.7840	0.2918	99.23	0.827
2.530	0.1075	0.3449	101.8	95.95	10.19	0.8151	0.3306	99.08	0.680
2.846	0.1107	0.3554	101.9	95.92	10.12	0.8190	0.3652	98.96	0.560
3.162	0.1136	0.3616	102.0	95.89	10.05	0.8105	0.4003	98.92	0.462
3.479	0.1155	0.3752	101.9	95.85	9.959	0.8238	0.4261	98.68	0.383
3.795	0.1174	0.3870	101.8	95.82	9.900	0.8015	0.4511	98.55	0.s20
4.111	0.1191	0.3986	101.8	95.79	9.844	0.7739	0.4733	98.44	0.269
4.427	0.1205	0.4052	101.8	95.76	9.791	0.7517	0.4999	98.41	0.228

Dependence of C_2 on A_1 and A_2

Perhaps the most interesting of all the eight parameters of the Chesler–Cram model is the slope C_2, of the hyperbolic tangent function. This quantity may be viewed as a measure of the peak broadness. As the value of C_2 increases, the tail of the peak becomes less pronounced. This we observed in our previous work, where we have described the elution profiles, of alkanes and alcohols. The C_2 values of the alcohols, which tailed severely, were smaller than those of the alkanes, which exhibited more symmetrical peaks.

Fig. 1 shows the dependence of C_2 on A_2 for two values of A_1. It is seen that, for each A_1 value, there exists a point of discontinuity in the C_2–A_2 plots. This was originally thought to be a convergence problem until it was noted that a similar behavior occurred with our experimental data[1] where hexane peaks were fitted to the Chesler–Cram equation. As will be shown, C_3, C_6 and C_8 also exhibit this peculiar behavior. The discontinuity, it should be noted, does not coincide with the

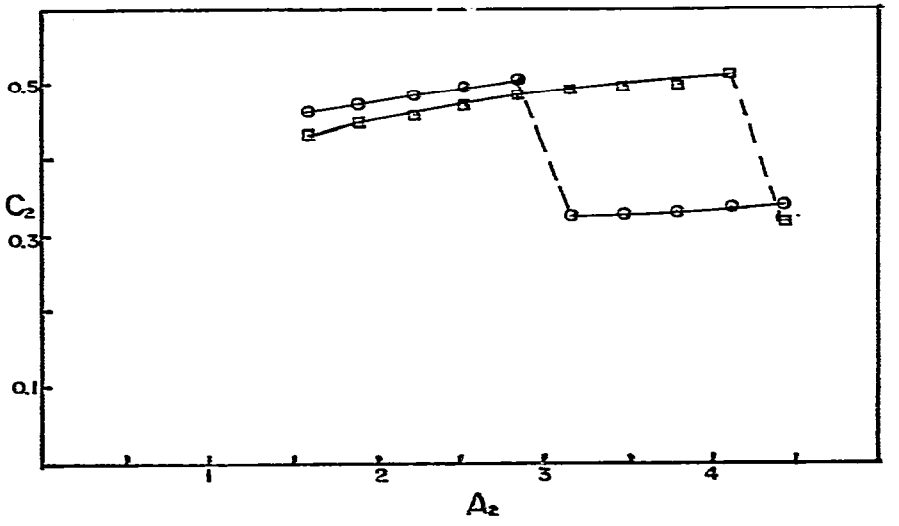

Fig. 1. C_2 *versus* A_2. The values of A_1 are 0.4 (○) and 1.1 (□). $t_m = 10$ sec. The solid and broken lines are drawn to show the trend of the data only. Broken lines indicate discontinuities.

position of the skew maximum. To examine in more detail the nature of the discontinuity, two peaks with S_2 values corresponding to each side of the discontinuity were plotted. These peaks were quite similar and gave no indication as to the nature of the discontinuity. On either side of the break, C_2 increased with an increase in A_2. This is expected since a large A_2 value indicates increased desorption rate, more symmetrical peaks and hence larger C_2 value.

Fig. 1 shows that the discontinuity shifts to larger A_2 values as A_1 is increased. An increase in A_1 at constant A_2 means that while the length of the tail remains the same, the relative concentration of the solute there decreases. The reason for the shift in the discontinuity as a function of A_1 is not clear to us at this point. It should be pointed out that as A_2 increases, C_2 decreases. The smaller magnitude of the tail is manifested in the Chesler–Cram model by a more gentle connection function with a flatter slope. An inspection of Fig. 1 and the tables reveals that a plot of C_2 *versus* A_1 at constant A_2 has also a discontinuity, the position of which (on the A_1 axis) is a function of A_2.

From Tables III and IV, the behavior of C_2 or of A_1 can be examined for the case were $t_m = 5$ sec. Since all other parameters are constant smaller t_m values mean larger k_a and k_d. As expected C_2 increases with A_2. Changing the magnitude of the rate constants does not change the trend in the peak shape. Note, however, that the position of the point of discontinuity is very much effected by the values of k_a and k_d.

Dependence of C_3 and C_8 on A_1 and A_2

Previous studies[1,2] have shown that C_3, the position in time of the midpoint of the hyperbolic tangent function, and C_8, the position in time where the exponential decay starts, should be considered together. We shall continue to look at these two quantities together in the present study as well.

Tables I and II show that for a given value of A_1 there is a discontinuity in C_3 and C_8 as a function of A_2. The position of the discontinuity on the A_2 axis is the same as in the C_2 case. Graphical examples of the dependence of C_3 and C_8 on A_2

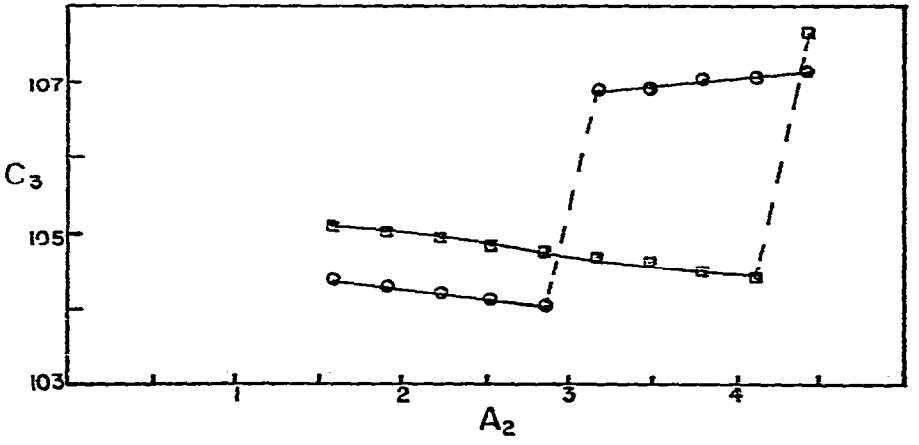

Fig. 2. C_3 *versus* A_2. The values of A_1 are 0.4 (○) and 1.1 (□). $t_m = 10$ sec. The solid and broken lines are drawn to show the trend of the data only. Broken lines indicate discontinuities.

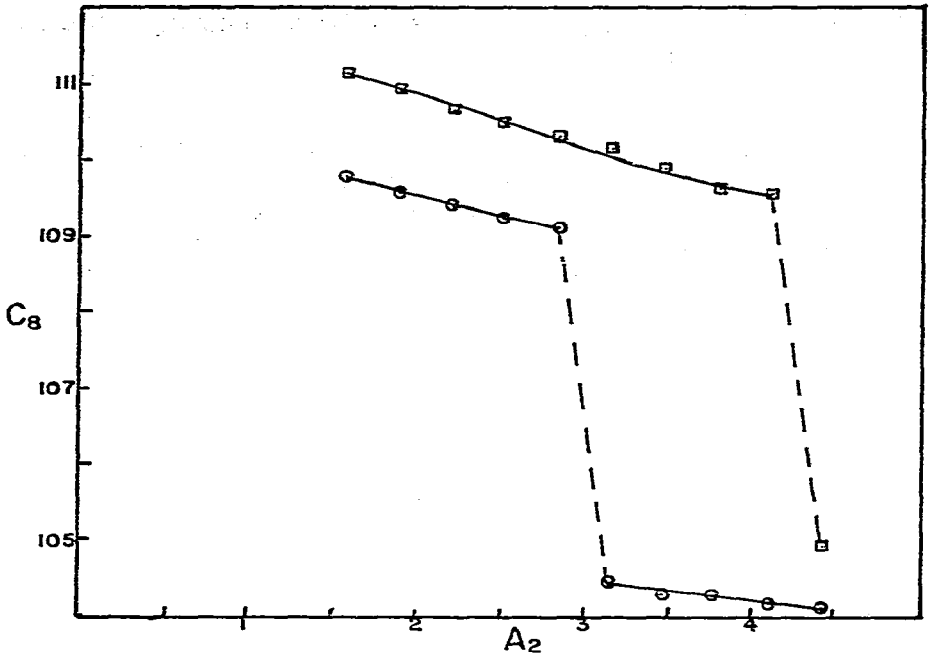

Fig. 3. C_8 *versus* A_2. The values of A_1 are 0.4 (○) and 1.1 (□). $t_m = 10$ sec. The solid and broken lines are drawn to show the trend of the data only. Broken lines indicate discontinuities.

are shown in Figs. 2 and 3. Several observations are striking. C_8 decreases continuously as A_2 is increased. C_3, on the other hand, decreases at low A_2 values up to the point of discontinuity. Past that point, C_3 increases as A_2 is increased. The decrease in C_3 and C_8 with increasing A_2 might be associated with the decreased importance of the tail.

At low A_2 values, before the point of discontinuity $C_8 > C_3$. The inverse is true past that point, where $C_3 > C_8$. The inversion in the order of C_3 and C_8 was also observed experimentally[1]. The reason for this inversion, which was not understood previously might, again, be tied to peak symmetry. It was observed that as A_1 is increased the point of discontinuity and of the inversion of C_3–C_8 occur at a lower skew value, indicating the importance of the symmetry. The change in the order of C_3 and C_8 with the peak shape is a peculiarity of the Chesler–Cram model. This behavior, however, can be utilized beneficially to extract physical parameters related to the chromatographic processes.

Increasing A_1 at a constant A_2 causes an increase (shifting toward longer time) of C_3 and C_8. There is, as might be expected, a discontinuity in C_3 and C_8 as a function of the adsorption rate constant, and all the arguments made previously hold true in this case. The change in C_3 and C_8, with the exception of the discontinuity point, is not very large.

Tables III and IV show the behavior of C_3 and C_8 for the case where $t_m = 5$ sec. At low A_1 value, C_3 increases slightly while C_8 decreases slightly as A_2 is increased. Moreover, $C_3 > C_8$. At a higher value of A_1 there is again a discontinuity in C_3 and C_8. Whereas before the discontinuity $C_3 > C_8$, the opposite is true past this point.

C_8 decreases slightly with increasing A_1 before and after the discontinuity, while C_3 goes through a shallow maximum.

Dependence of C_6 on A_1 and A_2

C_6 was the parameter of the Chesler–Cram equation which was responsible for the best fit of the empirical equation to a simulated Gaussian peak[1]. The value of this parameter was 10^{-8}. Since C_6 is the ratio of the height of the peak at $t = C_8$ (*i.e.*, where the exponential decay begins) to that of the peak maximum, such a small value made the contribution of the exponential decay negligible. It was therefore expected that as the peak symmetry increases and as the peaks approach a Gaussian shape, C_6 will decrease. Tables I–IV show that, in general, such is indeed the case. Not surprisingly, a discontinuity in C_6 as a function of either A_1 or A_2, exists. At low A_1 values, past the discontinuity point, C_6 increases with increasing A_2. The reason for this behavior is not immediately clear to us. As A_1 increases, so does C_6. This behavior is clear. The relative height of the tail portion of the peak increases with A_1 and therefore so does C_6. Fig. 4 shows the dependence of C_6 on A_2.

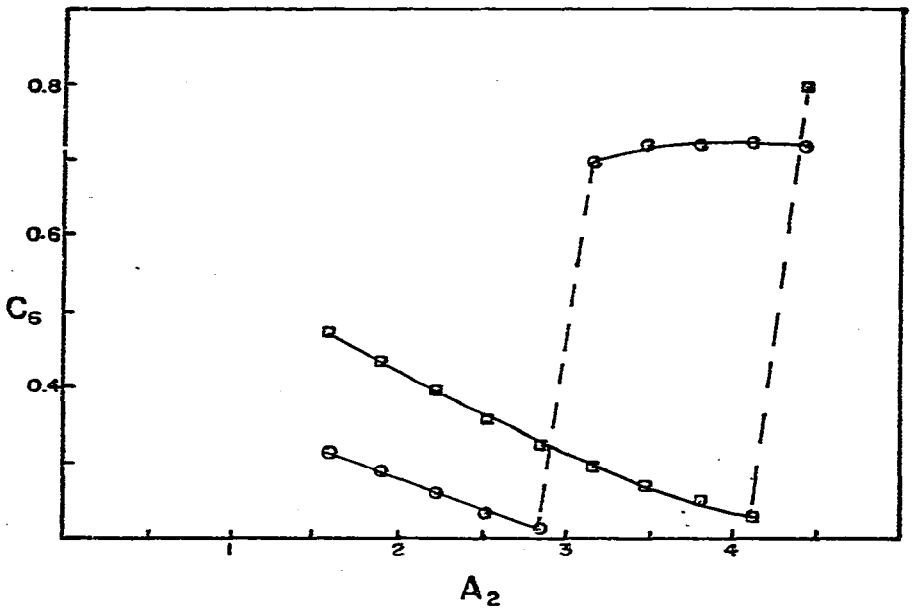

Fig. 4. C_6 *versus* A_2. The values of A_1 are 0.4 (○) and 1.1 (□). $t_m = 10$ sec. The solid and broken lines are drawn to show the trend of the data only. Broken lines indicate discontinuities.

Similar behavior of C_6 is observed when $t_m = 5$ sec.

As with the other parameters of the empirical model, C_6 cannot be discussed independently of the other parameters. Even though C_6 may be large, the peak may not be broad, or may not exhibit a long tail, if C_7 takes on a large value, causing the peak to rapidly decay to the baseline.

Dependence of C_7 on A_1 and A_2

The rate of the exponential decay, C_7, contributes, of course, to the width of

the back half of the peak. A large value of C_7 means a less pronounced tail, while a small value of this parameter indicates a slow and gentle decay. Tables I–IV show that C_7 increases with a decrease in A_1 and an increase in A_2. Typical behavior of C_7 is demonstrated in Fig. 5. It appears, at first glance, that there is no discontinuity in the behavior of C_7. Fig. 5, however, shows that such is not the case. A discontinuity does exist, but, relative to the behavior of the other parameters, the change accompanying it is small. We will assume, nonetheless, that as a first approximation, C_7 is a monotonic function. The dependence of C_7 on A_1 and on A_2 is well understood. An increase in A_2 or a decrease in A_1 is associated with a decreased importance of the tail portion of the peak. In the former case, the peak becomes more symmetrical, while in the latter, the relative height of the tail diminishes.

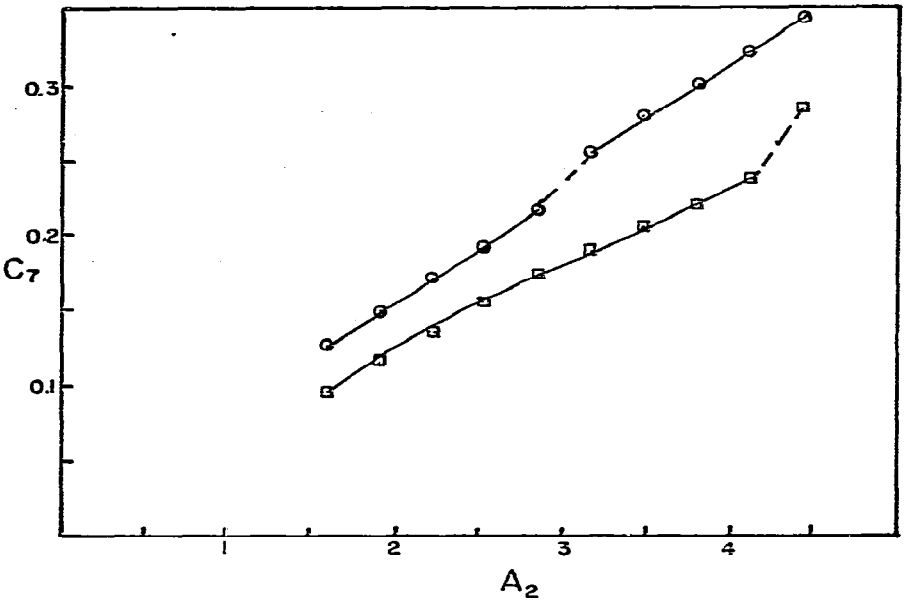

Fig. 5. C_7 *versus* A_2. The values of A_1 are 0.4 (○) and 1.1 (□). t_m = 10 sec. The solid and broken lines are drawn to show the trend of the data only. Broken lines indicate discontinuities.

The fact that C_7 seems to be a smooth function of the adsorption–desorption rate constant points to the possible utilization of this parameter in assigning values of A_1 and A_2 to experimental peaks. This will be discussed shortly.

Dependence of C_4 and C_5 on A_1 and A_2

Although these two parameters do not effect the shape of the back half of the peak, their dependence on the adsorption–desorption phenomena is of interest.

C_4, the position of the maximum of the Gaussian portion of the peak, should not be effected by A_1 and A_2. Tables I–IV illustrate that point; the change in C_4 is minimal indeed. C_5, on the other hand, changes to a greater extent with A_1 and A_2. As A_1 increases or as A_2 decreases, C_5 increases. The fact that C_5 does change with the adsorption–desorption rate is due to the fact that the Chesler–Cram constants are fitting parameters and are not true constants.

TABLE V

THE MOMENTS FOR PEAKS GENERATED FROM EQNS. 2 AND 3
$N = 1000$, $t_s = 90$ sec, $t_m = 10$ sec and $A_1 = 0.2$.

A_2	μ_1 (sec)	μ_2 (sec^2)
1.581	104.1	45.43
1.897	103.5	36.27
2.214	103.0	29.89
2.530	102.6	24.41
2.846	102.3	22.20
3.162	102.1	19.87
3.479	101.9	18.12
3.795	101.8	16.78
4.111	101.6	15.74
4.427	101.5	14.92

The Chesler–Cram Gaussian contribution to the peak shape should not be employed to extract any physical quantities. The first and second (central) moments are better indicators of the behavior of the retention time and variance as a function of A_1 and A_2. Table V shows examples of these moments for the case $t_m = 10$ sec,

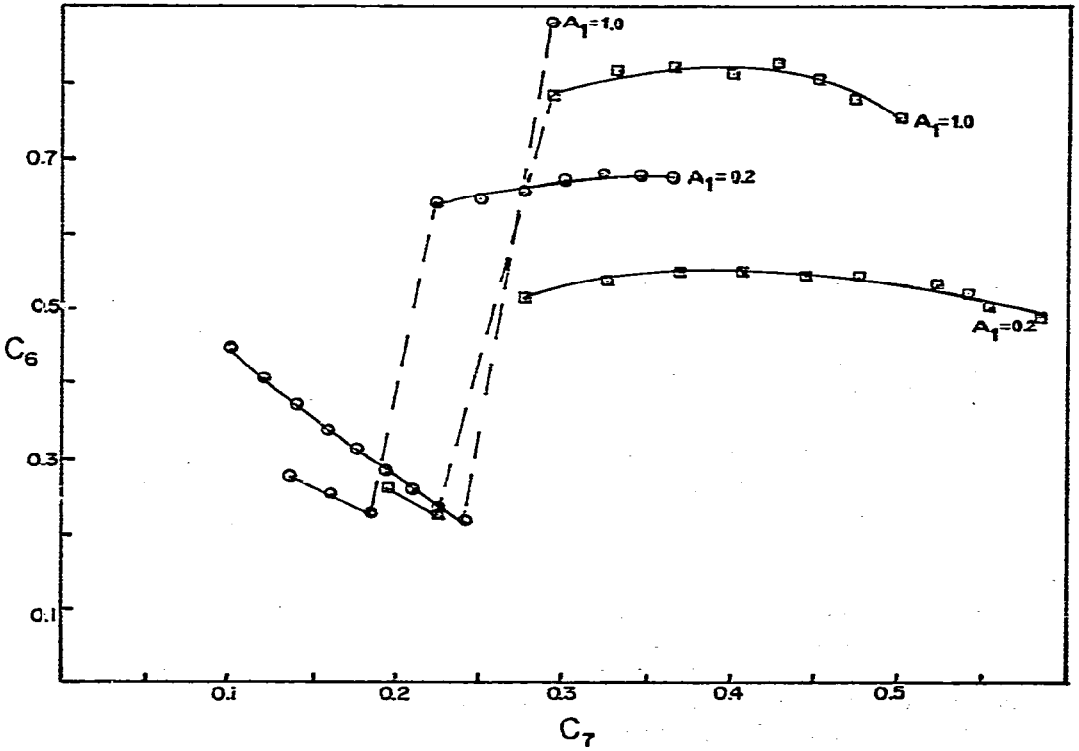

Fig. 6. Families of C_6 *versus* C_7 curves for several A_1 values. Each point on a curve corresponds to an A_2 value. The t_m values are 10 (○) and 5 (□) sec. The lines are drawn to show the trend of the data only. Broken lines indicate discontinuities.

$A_1 = 0.2$ and various values of A_2. The decrease in the two moments with increasing desorption rates is quite large. As A_2 increases, the tail becomes smaller and its contribution to the variance diminishes rapidly. Similar arguments hold true for the first moment. It should be noted that the numerical values of the true moments approach C_4 and C_5 as the peak symmetry improves.

CONCLUSIONS

There seems to be a correlation between the Chesler–Cram parameters and the adsorption–desorption rate constants in Giddings' stochastic model. This is quite promising since it means that the rate constant can be obtained with relative ease from experimental data via the Chesler–Cram empirical fitting equation. One possibility is to use plots such as shown in Figs. 1–5. A better method might be plotting two parameters such as shown in Fig. 6. Here C_6 is plotted *versus* C_7 for various A_2 values at constant A_1. The figure is a two-dimensional representation of a three-dimensional graph whose axes are C_6, C_7 and A_1. Fig. 6 seems to indicate that by knowing t_m and by obtaining C_6 and C_7 from the experimental peaks, A_1 and A_2 can be estimated quite accurately. These values of A_1 and A_2 can be used then as initial estimates in the theoretical model to gain more accurate adsorption–desorption rate constants.

Further studies are required to substantiate the findings presented here. The reasons for the choice of the empirical model over the stochastic one are in its ease of use. If, however, the empirical model is to be used, the significance of its parameters must be ascertained. In particular, the behavior of the skew and the presence of the discontinuities should be understood.

REFERENCES

1 S. D. Mott and E. Grushka, *J. Chromatogr.*, 126 (1976) 191.
2 S. D. Mott and E. Grushka, *J. Chromatogr.*, 148 (1978) 305.
3 S. N. Chesler and S. P. Cram, *Anal. Chem.*, 45 (1973) 1354.
4 J. C. Giddings and H. Eyring, *J. Phys. Chem.*, 59 (1955) 416.
5 R. A. Keller and J. C. Giddings, *J. Chromatogr.*, 3 (1960) 205.
6 J. C. Giddings, *Anal. Chem.*, 35 (1963) 1999.
7 J. C. Giddings, *Dynamics of Chromatography*, Marcel Dekker, New York, 1965.
8 D. A. McQuarrie, *J. Chem. Phys.*, 38 (1963) 437.
9 C. Vidal-Madjar and G. Guiochon, *J. Chromatogr.*, 142 (1977) 61.